Available online at www.sciencedirect.com
ScienceDirect
Journal of Solid State Chemistry 181 (2008) 539–551
JOURNAL OF SOLID STATE CHEMISTRY
www.elsevier.com/locate/jssc

Mononuclear, trinuclear, and hetero-trinuclear supramolecular complexes containing a new tri-sulfonate ligand and cobalt(II)/copper(II)-(1,10-phenanthroline)$_2$ building blocks

Yunfang Yu[a], Yongqin Wei[a], Ria Broer[b], Rongjian Sa[a], Kechen Wu[a,*]

[a]*State Key Laboratory of Structural Chemistry, Fujian Institute of Research on the Structure of Matter, Chinese Academy of Sciences, Fujian 350002, China*
[b]*Zenike Institute for Advanced Materials, Rijksuniversiteit Groningen, Nijenborgh 4, 9747 AG Groningen, The Netherlands*

Received 29 September 2007; received in revised form 19 December 2007; accepted 27 December 2007
Available online 1 January 2008

Abstract

Novel mononuclear, trinuclear, and hetero-trinuclear supermolecular complexes, $[Co(phen)_2(H_2O)(HTST)]\cdot 2H_2O$ (**1**), $[Co_3(phen)_6(H_2O)_2(TST)_2]\cdot 7H_2O$ (**2**), and $[Co_2Cu(phen)_6(H_2O)_2(TST)_2]\cdot 10H_2O$ (**3**), have been synthesized by the reactions of a new tri-sulfonate ligand (2,4,6-tris(4-sulfophenylamino)-1,3,5-triazine, H_3TST) with the M^{2+} (M = Co, Cu) and the second ligand 1,10-phenanthroline (phen). Complex **1** contains a *cis*-Co(II)(phen)$_2$ building block and an HTST as monodentate ligand; complex **2** consists of two TST as bidentate ligands connecting one *trans*- and two *cis*-Co(II)(phen)$_2$ building blocks; complex **3** is formed by replacing the *trans*-Co(II)(phen)$_2$ in **2** with a *trans*-Cu(II)(phen)$_2$, which is the first reported hetero-trinuclear supramolecular complex containing both the Co(II)(phen)$_2$ and Cu(II)(phen)$_2$ as building blocks. The study shows the flexible multifunctional self-assembly capability of the H_3TST ligands presenting in these supramolecular complexes through coordinative, H-bonding and even π–π stacking interactions. The photoluminescent optical properties of these complexes are also investigated and discussed as well as the second-order nonlinear optical properties of **1**.

Keywords: Supermolecule; Cobalt; Copper; Luminescent; Nonlinear optics; Ab initio

1. Introduction

In recent years the design and synthesis of supramolecular coordination framework structures have attracted great attentions in which the coordinative, hydrogen bonding, and π–π stacking interactions are widely employed [1–5]. With the development of self-assembly supramolecular chemistry, the rational design and synthesis of supramolecular architectures based on covalent or supermolecular interactions have been an important content of coordination chemistry and have been found applications in searching novel materials with catalytic, biological, and photophysical properties such as luminescent and nonlinear optical properties [6,7]. However, finding appropriate molecular materials from organic ligands and transition metals building blocks to construct novel supramolecular architectures are still a challenge to chemists [6].

As organic ligands, sulfonate ligands are possible to afford coordinative [8–10] and hydrogen bonding interactions [11]. In the past years some studies have been reported with organic sulfonate ligands towards transition metals in the field of supramolecular chemistry, especially the studies with rigid bi- and tri-sulfonate ligands [12–15]. However, comparing to aromatic polycarboxylate ligands, the coordination chemistry of sulfonate ligands is less explored owing to their relatively weak coordination ability [16]. The supramolecular complex systems containing flexible tri-sulfonate ligands and hetero-metal building blocks are limited reported as well [17].

In order to study the coordination information of flexible tri-sulfonate ligand and its behaviors in the construction of supramolecular architectures, we designed

*Corresponding author. Fax: +86 591 8379 2932.
E-mail address: wkc@fjirsm.ac.cn (K. Wu).

0022-4596/$ - see front matter © 2007 Elsevier Inc. All rights reserved.
doi:10.1016/j.jssc.2007.12.028

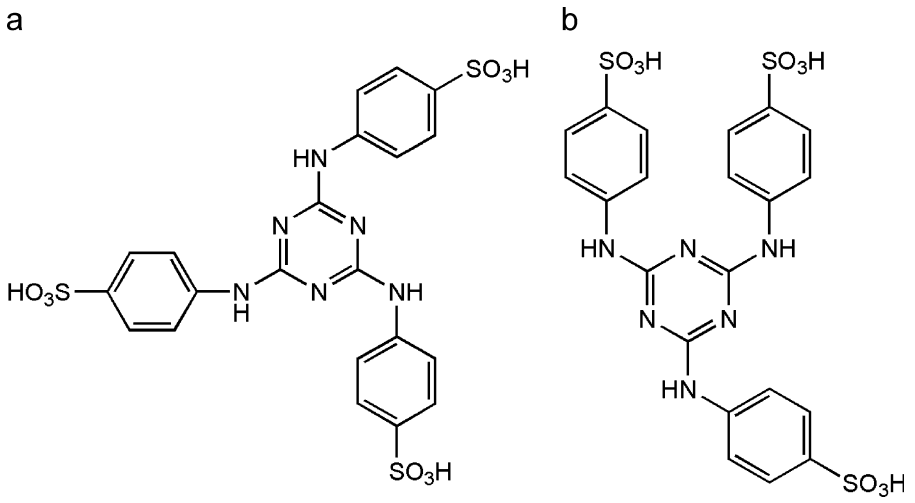

Scheme 1. Two possible conformations of H_3TST: (a) Δ-conformation and (b) φ-conformation.

and synthesized a new tri-sulfonate ligand, namely H_3TST = 2,4,6-tris(4-sulfophenylamino)-1,3,5-triazine. This ligand is a flexible aromatic ligand with three SO_3H groups which are located at the end of molecule "arms" that can rotate around the C–NH–C bonds. Through this rotation it has two different possible conformations, Δ and φ, as shown in Scheme 1. Besides the three sulfonate groups in tri-sulfonate ligand, the three N–H groups and the aromatic rings of triazine and phenyl groups are also helpful to construct supramolecular architectures.

By using H_3TST and 1,10-phenanthroline (phen) as ligands, we synthesized three new transition metal supermolecular complexes, $[Co(phen)_2(H_2O)(HTST)]\cdot 2H_2O$ **1**, $[Co_3(phen)_6(H_2O)_2(TST)_2]\cdot 7H_2O$ **2**, and $[Co_2Cu(phen)_6(H_2O)_2(TST)_2]\cdot 10H_2O$ **3**, which presented mononuclear, trinuclear, and hetero-trinuclear architectures, respectively. The latter is the first reported hetero-metallic supramolecular complex containing both $Co(II)(phen)_2$ and $Cu(II)(phen)_2$ building blocks. These three supermolecular complexes also illustrate the coordination chemistry of tri-sulfonate TST/HTST ligands toward $Co(II)/Cu(II)(phen)_2$ building blocks in the aqueous solution and their contributions in supramolecular self-assembly techniques.

The special photophysical properties of the supermolecular architectures containing transition metals have attracted great interests due to the various features of the linear and nonlinear optical responses. The rational design of the supermolecular chromophores with large molecular hyperpolarizability mainly organometallic dipolar chromophores encourages the present study. The first hyperpolarizability of one of the three complexes was experimentally determined and theoretically analyzed to understand the structure–property relationship, which may benefit to the further novel optical material developments.

2. Experimental section

2.1. Materials and measurements

All commercially available solvents and starting materials were used as received without further purification. Elemental analyses (C, H, and N) were performed with a Vario EL III CHNOS Elemental Analyzer. Metal elemental analysis of complex **3** was carried out on an Ultima-2 ICP Emission Spectrometer. The infrared spectrum of KBr pellet was recorded on a Perkin-Elmer Spectrum One FT-IR Spectrometer. The emission spectrum was recorded on an FLS920 fluorescence spectrophotometer. Thermogravimetric analyses (TGA) were carried out under an N_2 atmosphere at a heating rate of 15 °C/min. The HRS measurement was performed with a pulsed Nd: YAG laser at 1.064 μm. Solution of the sample in DMSO was used with *p*-nitroaniline as a reference. The weak contributions of two-photon induced fluorescence in the HRS measurements were directly subtracted to HRS signal as background noises using a high-resolution monochromator near 532 nm.

2.2. Preparation of $H_3TST\cdot 7H_2O$

A solution of 4-aminobenzenesulfonic sodium (14.72 g, 0.075 mol) in 200 ml water was added dropwise into cyanuric chloride (4.61 g, 0.025 mol) in 100 ml acetone at 0–5 °C under stirring. After 1 h, the mixture was heated to 45 °C and reacted under stirring for 8 h. After cooling, white deposit $H_3TST\cdot 7H_2O$ was filtered from the mixture, washed with acetone and water, oven-dried at 60 °C in 76% yield. Anal. calc. for $H_3TST\cdot 7H_2O$: C 34.99, H 4.48, N 11.66; found: C 35.03, H 4.39, N 11.73. ^{1}H NMR (DMSO): N–H 9.664, phenyl 7.714 7.570, H_2O 3.913. IR (KBr pellet, cm^{-1}): 3452(b), 1631(s), 1588(s), 1561(s), 1509(s), 1493(s), 1412(m), 1378(w), 1335(w), 1190(s), 1130(s), 1068(w),

1037(s), 1009(s), 835(m), 772(w), 751(w), 709(m), 682(m), 625(w), 599(m), 567(m).

2.3. Preparation of $[Co(phen)_2(H_2O)(HTST)]\cdot 2H_2O$ (1)

This compound was synthesized by the hydrothermal method from a mixture of $H_3TST\cdot 7H_2O$ (0.072 g, 0.1 mmol), phen$\cdots H_2O$ (0.059 g, 0.3 mmol), $CoCl_2$ (0.039 g, 0.3 mmol) and water (20.0 mL) in a 25.0 mL Teflon-lined stainless steel reactor. The solution was heated at 160 °C for three days, and then the reactor was slowly cooled to room temperature to give orange crystals of **1** in 57% yield. Anal. calc. for $C_{45}H_{38}CoN_{10}O_{12}S_3$: C 50.66, H 3.56, N 13.13; found: C 50.58, H 3.52, N 13.07.

2.4. Preparation of $[Co_3(phen)_6(H_2O)_2(TST)_2]\cdot 7H_2O$ (2)

This compound was synthesized under the same conditions by the hydrothermal method, except for the reactants of $H_3TST\cdot 7H_2O$ (0.072 g, 0.1 mmol), phen$\cdots H_2O$ (0.119 g, 0.6 mmol), $CoCl_2$ (0.039 g, 0.3 mmol) and water (20.0 mL), and red crystals of **2** were produced in 53% yield. Anal. calc. for $C_{114}H_{96}Co_3N_{24}O_{27}S_6$: C 52.55, H 3.69, N 12.91; found: C 52.49, H 3.66, N 12.93.

2.5. Preparation of $[Co_2Cu(phen)_6(H_2O)_2(TST)_2]\cdot 10H_2O$ (3)

This compound was also synthesized under the same conditions by the hydrothermal method, except for the reactants of $H_3TST\cdot 7H_2O$ (0.072 g, 0.1 mmol), phen$\cdots H_2O$ (0.119 g, 0.6 mmol), $CoCl_2$ (0.026 g, 0.2 mmol), $CuCl_2\cdot 2H_2O$ (0.017 g, 0.1 mmol) and water (20.0 mL), and green crystals of **3** were produced in 36% yield. Anal. calc. for $C_{114}H_{102}Co_2CuN_{24}O_{30}S_6$: C 50.66, H 3.56, N 13.13, Co 4.43, Cu 2.39; found: C 50.58, H 3.52, N 13.07, Co 4.37, Cu 2.35.

2.6. Crystallography

The X-ray diffraction measurements for complexes **1**–**3** were carried out on a Rigaku Mercury CCD diffractometer with graphite-monochromatized Mo$K\alpha$ radiation. The structures were solved by direct methods and refined on F^2 by full-matrix least-squares technique using the SHELX97 program package [18]. In complex **2**, the trans-$Co(phen)_2O_2$ group and five water molecules are disordered, and the C81, C82, C83, C84, C85, C86, C88, C90, C91, C92, C93, C94, C95, C96, C98, C100, O2w, O3w, O4w, O5w, and O6w were treated with a site occupation factor of 0.5. Anisotropic thermal parameters were applied to all nonhydrogen atoms. In complex **1**, all hydrogen atoms were located from Fourier map. In complex **2**, the hydrogen atoms of disordered atoms could not be located, and other hydrogen atoms were generated geometrically except for those on O10 and O1w, which were taken from Fourier map. In complex **3**, the hydrogen atoms were generated geometrically except for those of water molecules, which were taken from Fourier map. The crystallographic data are listed in Table 1. CCDC −648026 to −648028 (for compounds **1**, **2**, and **3**, respectively) contain the supplementary crystallographic data for this paper. These data can be obtained free of charge from The Cambridge Crystallographic Data Centre via http://www.ccdc.cam.ac.uk/data_request/cif.

2.7. Computational detail

All theoretical calculations of complex **1** were performed by using the Gaussian 03 program package [19]. In view of the open-shell system and the electron configuration of cobalt (II), spin-unrestricted calculations were carried out and the spin multiplicity was set to 4. The initial structure was taken from the X-ray crystallographic data. The electronic structure was calculated by using the hybrid functional PBE1PBE and the Los Alamos relativistic ECP basis set LanL2MB. The electronic transitions were computed by means of TDDFT method at the same level of theory, namely, UPBE1PBE/LanL2MB. The static first hyperpolarizability was evaluated by employing finite-field (F-F) approach, in which the uniform external electric field with strength of 0.0010 au was adopted. For comparison between the calculated and experimental results, the HRS measured frequency-dependent first hyperpolarizability β was extrapolated to zero frequency one β_0 by means of the two-level model (TLM):

$$\beta_0 = \beta_\omega\left(1-\frac{4\lambda_{\max}^2}{\lambda^2}\right)\left(1-\frac{\lambda_{\max}^2}{\lambda^2}\right).$$

And then the theoretical orientation-averaged first hyperpolarizability was calculated by using the following formulas by Cyvin et al. [20]:

$$\langle\beta_{HRS}^2\rangle = \langle\beta_{ZZZ}^2\rangle + \langle\beta_{XZZ}^2\rangle,$$

$$\langle\beta_{ZZZ}^2\rangle = \frac{1}{7}\sum_i\beta_{iii}^2 + \frac{6}{35}\sum_{i\neq j}\beta_{iii}\beta_{ijj} + \frac{9}{35}\sum_{i\neq j}\beta_{ijj}^2 + \frac{6}{35}\sum_{ijk,\text{cyclic}}\beta_{ijj}\beta_{jkk} + \frac{12}{35}\beta_{ijk}^2,$$

$$\langle\beta_{XZZ}^2\rangle = \frac{1}{35}\sum_i\beta_{iii}^2 + \frac{2}{105}\sum_{i\neq j}\beta_{iii}\beta_{ijj} + \frac{11}{105}\sum_{i\neq j}\beta_{ijj}^2 - \frac{2}{105}\sum_{ijk,\text{cyclic}}\beta_{ijj}\beta_{jkk} + \frac{8}{35}\beta_{ijk}^2, \quad i,j,k = x,y,z.$$

3. Results and discussion

3.1. Synthesis

It is well known that chlorine atoms in cyanuric chloride could be easily replaced by other organic groups [21–23].

Table 1
Crystallographic data for the three complexes

	1	2	3
Empirical formula	$C_{45}H_{38}CoN_{10}O_{12}S_3$	$C_{114}H_{96}Co_3N_{24}O_{27}S_6$	$C_{114}H_{102}Co_2CuN_{24}O_{30}S_6$
Formula weight	1065.96	2603.30	2661.96
Crystal size (mm^3)	$0.45 \times 0.15 \times 0.15$	$0.34 \times 0.24 \times 0.22$	$0.30 \times 0.25 \times 0.14$
Crystal color	Orange	Red	Green
Crystal system	Triclinic	Monoclinic	Monoclinic
Space group	*P-1*	*C2/c*	*C2/c*
a (Å)	8.2460(2)	13.6452(15)	41.001(8)
b (Å)	11.744	23.563(3)	13.760(3)
c (Å)	24.1682(6)	35.729(5)	22.989(5)
α (deg)	76.121(6)	90.00	90.00
β (deg)	84.776(7)	95.078(2)	120.3400(10)
γ (deg)	75.536(5)	90.00	90.00
V ($Å^3$)	2198.92(8)	11,443(2)	11,194(4)
Z	2	4	4
$D_{calcd.}$ ($g\,cm^{-3}$)	1.611	1.512	1.580
$F(000)$	1098	5260	5492
μ (mm^{-1})	0.612	0.627	0.687
θ for data collection (deg)	2.20–27.48	2.29–27.48	2.04–27.48
Reflections collected	17163	42974	42105
Unique reflections	9935	13004	12780
(R(int))	[R(int) = 0.0210]	[R(int) = 0.0298]	[R(int) = 0.0295]
Parameters	792	888	809
GOF	1.054	1.088	1.090
$R1$, $wR2$ ($I > 2\sigma(I)$)	0.0456, 0.0988	0.0647, 0.1909	0.0533, 0.1262
$R1$, $wR2$ (all data)	0.0572, 0.1072	0.0744, 0.2034	0.0665, 0.1361

$R1 = \sum(|F_o|-|F_c|)/\sum|F_o|$, $wR2 = [\sum w(F_o^2-F_c^2)^2/\sum w(F_o^2)^2]0.5$.

The ligand H_3TST was prepared by reaction of cyanuric chloride with 4-aminobenzenesulfonic sodium in mixed CH_3COCH_3/H_2O solvent. Because H_3TST is only slightly dissolved in water, it is easily to wash off the impurities with water and acetone.

Hydrothermal reaction was adopted in the syntheses of the complexes. Keeping in mind of the weak coordination ability of sulfonate anions towards transition metals in aqueous environment [17], and the reports of Cai et al. [12–14], which stated that sulfonate anion can compete with water molecules and coordinate directly to transition metals when introducing suitable nitrogen-containing auxiliaries to the metal center, we selected 1,10-phenanthroline (phen) as the second ligand and obtained the three complexes.

Complexes **1** and **2** were prepared with nearly the same reactants, expect for the quantity of phen in the reaction. When the phen was double of that added in the preparation of complex **1**, the red crystal of **2** was generated, instead of the orange crystal of **1**. And it was found that complex **2** could also be obtained when half of the phen reactant (3 mmol) was replaced by NaOH (1 mmol) in the reaction. In fact, TST ligand exists in the form of $HTST^{2-}$ in complex **1** and TST^{3-} in complex **2** when more base (phen or NaOH) is added. This difference of deprotonation indicates that the self-assembly of complex **1** or **2** is determined by the quantity of base in the reaction.

In the preparation of **3**, using $CuCl_2$ to replace $\frac{1}{3}$ $CoCl_2$ reactant in **2**, the green crystal of **3** was obtained by introducing $Cu(phen)_2$ unit into the complex, and there was no crystal of **2** observed.

Another notable thing is that no crystal constructed by only Cu metal atom and the two ligands was obtained in our study though many experimental methods have been tried.

3.2. Crystal structures

3.2.1. Coordination geometry of Co(II) and Cu(II) centers

The Co(II) and Cu(II) cations in the three complexes are all octahedrally coordinated with the four nitrogen atoms of the phen ligands and the two oxygen atoms of SO_3^- groups or aqua ligands to form MN_4O_2 (M = Co(II), Cu(II)) moiety. There are two coordination modes as shown in Scheme 2. One is the *cis*-fashion of $Co(phen)_2O_2$ in **1**, $Co1(phen)_2O_2$ in **2** and $Co(phen)_2O_2$ in **3**, with one of the oxygen atoms of SO_3^- group and the other of aqua ligand. The other mode is the *trans*-fashion in $Co2(phen)_2O_2$ in **2** and $Cu(phen)_2O_2$ in **3** coordinated with the two oxygen atoms of SO_3^- groups. The distances between Co(II) and the coordinate sulfonate oxygen are consistent (2.1–2.2 Å), but the distances between Cu(II) and coordinate sulfonate oxygen (2.868(5) Å) in **3** are influenced by Jahn–Teller effect [24]. Selected bond lengths and angles for **1**, **2** and **3** are listed in Table 2.

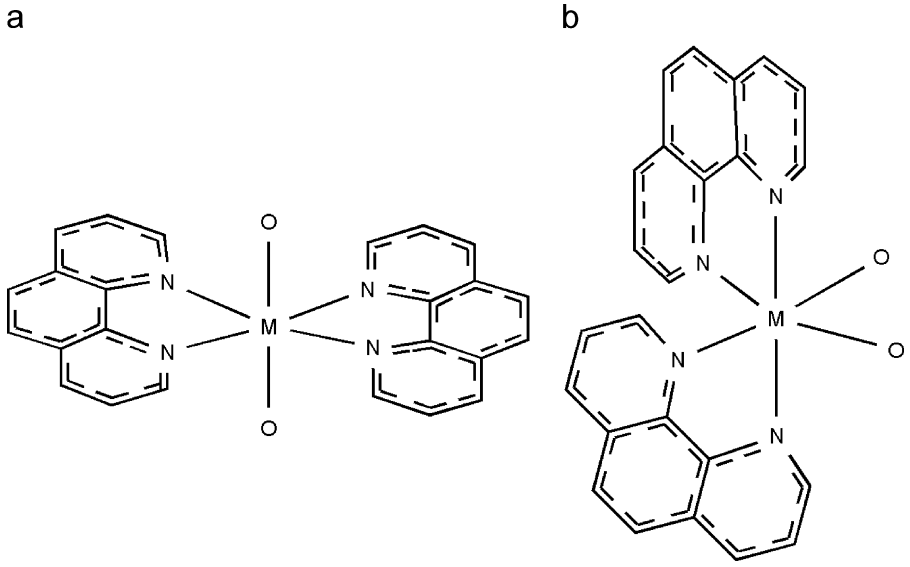

Scheme 2. Two coordination modes of Co(II)/Cu(II)(phen)$_2$O$_2$: (a) *trans*-fashion and (b) *cis*-fashion.

Table 2
Selected bond lengths and angles (unit: Å and deg) for **1**–**3**

Compound **1**					
Co–N1	2.112(2)	Co–N3	2.129(2)	Co–O1	2.1238(16)
Co–N2	2.132(2)	Co–N4	2.1347(19)	Co–O1w	2.112(2)
N1–Co–N2	78.51(8)	N2–Co–N3	102.70(7)	N3–Co–O1w	87.25(8)
N1–Co–N3	97.44(8)	N2–Co–N4	92.79(7)	N4–Co–O1	95.53(7)
N1–Co–N4	169.33(9)	N2–Co–O1w	169.76(8)	N4–Co–O1w	91.59(8)
N1–Co–O1	89.59(7)	N3–Co–N4	78.31(8)	O1–Co–O1w	87.20(8)
N1–Co–O1w	98.01(9)	N3–Co–O1	171.59(7)		
Compound **2**					
Co1–N7	2.136(3)	Co1–O8	2.157(2)	Co2–N13	2.164(4)
Co1–N8	2.170(3)	Co1–O10	2.052(3)	Co2–N14	2.199(5)
Co1–N9	2.156(3)	Co2–N11	2.118(5)	Co2–O4	2.132(2)
Co1–N10	2.121(3)	Co2–N12	2.172(4)		
N7–Co1–N8	77.65(13)	O4–Co2–N11	91.05(14)	N11–Co2–N11^a	144.0(3)
N7–Co1–N9	93.59(13)	O4–Co2–N11^a	89.30(14)	N11–Co2–N12	71.98(13)
N7–Co1–N10	163.47(12)	O4–Co2–N12	90.56(6)	N11–Co2–N13	108.02(13)
N7–Co1–O8	98.57(10)	O4–Co2–N13	89.44(6)	N11–Co2–N14	177.12(18)
N7–Co1–O10	96.80(12)	O4–Co2–N14^a	86.42(14)	N11–Co2–N14^a	34.76(18)
N8–Co1–N9	101.89(11)	O4–Co2–N14^a	93.26(14)	N12–Co2–N13	180.000(1)
N8–Co1–N10	90.32(13)	O4–Co2–O4^a	178.88(11)	N12–Co2–N14	106.65(13)
N8–Co1–O8	82.15(9)	N9–Co1–O10	90.85(11)	N13–Co2–N14	73.35(13)
N8–Co1–O10	166.33(11)	N10–Co1–O8	90.85(10)	N14–Co2–N14^a	146.7(3)
N9–Co1–N10	77.67(14)	N10–Co1–O10	97.32(13)		
N9–Co1–O8	167.77(11)	O8–Co1–O10	86.40(9)		
Compound **3**					
Co–N3	2.122(2)	Co–N6	2.096(2)	Cu–N1	1.996(2)
Co–N4	2.135(2)	Co–O8	2.1092(19)	Cu–N2	1.993(2)
Co–N5	2.120(2)	Co–O10	2.179(2)	Cu–O3	2.868(4)
N3–Co–N4	78.35(10)	N4–Co–O10	172.39(9)	N2–Cu–N1	160.76(10)
N3–Co–N5	174.60(9)	N5–Co–N6	79.30(9)	N2–Cu–N1^b	99.56(9)
N3–Co–N6	99.29(9)	N5–Co–O8	93.95(9)	N2–Cu–N2^b	84.14(14)
N3–Co–O8	87.84(9)	N5–Co–O10	90.47(9)	O3–Cu–N1	86.32(4)
N3–Co–O10	94.66(9)	N6–Co–O8	171.91(9)	O3–Cu–N1^b	103.13(8)
N4–Co–N5	96.61(9)	N6–Co–O10	86.60(9)	O3–Cu–N2	74.48(8)
N4–Co–N6	97.42(9)	O8–Co–O10	89.03(9)	O3–Cu–N2^b	96.05
N4–Co–O8	87.72(9)	N1–Cu–N1^b	83.21(13)		

Symmetry code for **1–3**: (a) 2–x, y, $\frac{1}{2}$–z; (b) –x, y, $\frac{1}{2}$–z.

3.2.2. Monocobalt complex $[Co(phen)_2(H_2O)(HTST)]\cdot 2H_2O$ **1**

The $HTST^{2-}$ ligand exists as a negative divalent ion in the φ-conformation with the other two uncoordinated SO_3^- groups and a hydrogen atom from the neighboring unit is transferred to a nitrogen atom N7 of triazine ring. The strong H-bond (O1w···H–O3, 2.695(3) Å, shown in Table 3) linking the coordinated SO_3^- group and the aqua ligand stabilizes the coordination environment as shown in Fig. 1. One phen group forms a slipped intramolecular π–π stack (3.62 Å) with the phenyl ring of the coordinated sulfophenyl group of $HTST^{2-}$ ligand.

Intermolecular H-bonds (O1w···H–$O4^{\#1}$, 2.739(3) Å; N8–H···$O9^{\#1}$, 2.890(3) Å, shown in Table 3) are formed between neighboring molecules and connect them into a dimer unit, which is further confirmed by slipped π–π stacks (3.48 Å) between triazine and phenyl rings of the two $HTST^{2-}$ ligands. The dimers are then joined together by intermolecular N7–H···$O8^{\#2}$···H–N9 bonds (N7···$O8^{\#2}$, 2.849(2) Å; N9···$O8^{\#2}$, 2.867(3) Å; N7···$O8^{\#2}$···N9, 46.8°, shown in Table 3) between SO_3^- groups and nitrogen atoms from triazine and NH groups, yielding 1-dimensional (1D) chains, as shown in Fig. 2a. The *cis*-$Co(phen)_2O_2$ blocks are also arranged into 1D rows by face-to-face (3.34 Å) and point-to-face (3.44 Å) π–π interactions, which join the 1D chains into 2-dimensional (2D) supramolecular structure as shown in Fig. 2a and b.

Table 3
Hydrogen bonding interactions (unit: Å and deg) in **1**

D–H···A	D–H	H···A	D···A	D–H···A
N7–H12···$O8^{\#2}$	0.81(3)	2.11(3)	2.849(2)	151(2)
N8–H18···$O9^{\#1}$	0.81(3)	2.12(3)	2.890(3)	161(3)
N9–H10···$O8^{\#2}$	0.83(3)	2.07(3)	2.867(3)	162(3)
N10–H3···$O2w^{\#3}$	0.90(3)	2.08(3)	2.978(3)	175(2)
O1w–H1A···$O4^{\#1}$	0.77(4)	1.99(4)	2.739(3)	163(3)
O1w–H2A···O5	0.77(4)	2.00(4)	2.768(4)	178(4)
O1w–H2B···O3w	0.86(5)	2.29(5)	3.051(4)	147(4)
O1w–H3A···$O9^{\#4}$	0.92(7)	2.13(7)	3.042(4)	172(6)
O1w–H3B···O6	0.84(6)	2.12(6)	2.931(4)	162(5)
O1w–H1B···O3	0.90(5)	1.84(5)	2.695(3)	158(4)

Symmetry code: (#1) $-x+2$, $-y$, $-z+1$; (#2) $x-1$, $y+1$, z; (#3) $-x+3$, $-y$, $-z+1$; (#4) x, $y+1$, z.

3.2.3. Tricobalt cluster $[Co_3(phen)_6(H_2O)_2(TST)_2]\cdot 7H_2O$ **2**

The molecular of complex **2** has three Co centers as shown in Fig. 3, two of them (Co1) adopt the *cis* coordination mode which is similar to the Co center in **1** and the other one (Co2) is six coordinated in the *trans*-fashion by four nitrogen atoms from two phen groups and two SO_3^- oxygen atoms of the two

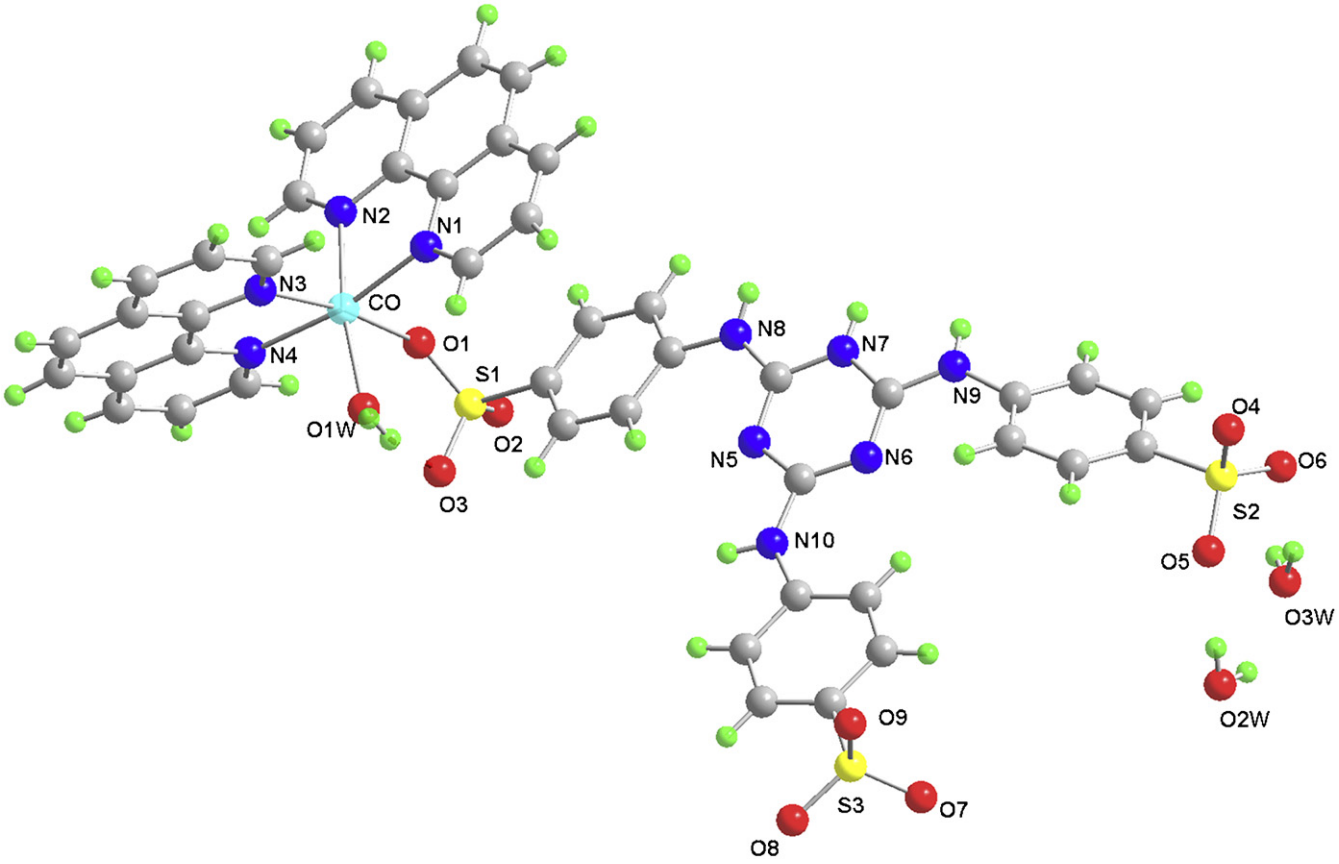

Fig. 1. The mononuclear complex molecule in **1**.

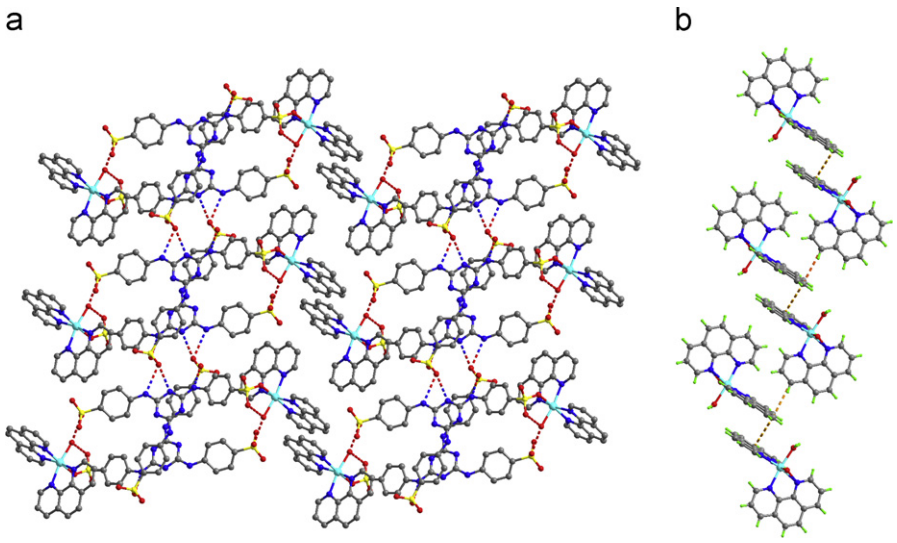

Fig. 2. (a) The 1D chains joined by 1D *cis*-Co(phen)$_2$O$_2$ rows yielding 2D supramolecular structure; (b) The 1D *cis*-Co(phen)$_2$O$_2$ row formed via π–π interactions in **1**.

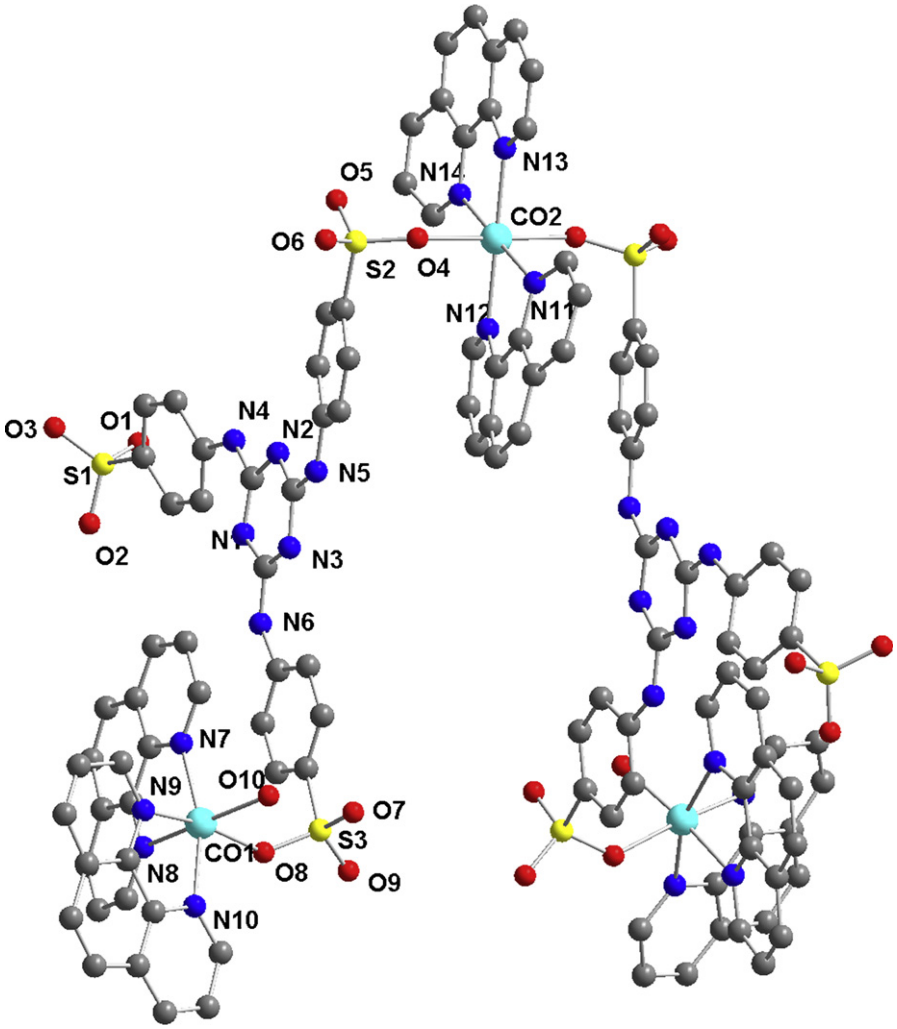

Fig. 3. The trinuclear cluster in **2**. Solvent water molecules and hydrogen atoms are omitted for clarity. Note that the *trans*-Co$_2$(phen)$_2$ group is disordered over two sites and only one is being shown for clarity.

TST^{3-} anions. Instead of the φ-conformation $HTST^{2-}$ in **1**, two Δ-conformation TST^{3-} groups connect two Co1 atoms and Co2 atom as bidentate ligands resulting a trinuclear cluster with intramolecular π–π interactions between phen and TST^{3-} groups. It is notable that the two phen molecules of *trans*-$Co2(phen)_2O_2$ form a slightly distorted planar motif, which has never been seen in $Co(phen)_2O_2$ units in CCDC.

Table 4
Hydrogen bonding interactions (unit: Å and deg) in **2**

D–H···A	D–H	H···A	D···A	D–H···A
N4–H4A···O9$^{\#1}$	0.88	2.18	2.999(3)	155.0
N5–H5B···O1$^{\#2}$	0.88	2.18	3.049(4)	170.5
N6–H6B···O4$^{\#3}$	0.88	2.46	3.219(3)	144.8
N6–H6B···O6$^{\#3}$	0.88	2.42	3.227(3)	151.7
O1w–H1A···O5$^{\#4}$	0.91(6)	1.97(6)	2.850(4)	162(5)
O1w–H1B···O2$^{\#5}$	0.94(5)	1.84(5)	2.769(4)	171(5)
O10–H10A···O7	0.84	1.89	2.712(3)	164.6
O10–H10B···O1w$^{\#6}$	0.77(6)	1.92(6)	2.687(4)	175(6)

Symmetry code: (#1) $x+1/2$, $y-\frac{1}{2}$, z; (#2) $x-1$, y, z; (#3) $x+\frac{1}{2}$, $y+\frac{1}{2}$, z; (#4) $-x+\frac{3}{2}$, $-y+\frac{1}{2}$, $-z$; (#5) $-x+2$, $-y+1$, $-z$; (#6) $-x+1$, $-y+1$, $-z$.

An extended 2D structure is constructed along *a* and *b* axes via intermolecular H-bonds between SO_3^- and H–N groups from TST^{3-} ligands (N4···O9$^{\#1}$, 2.999(3) Å; N5···O1$^{\#2}$, 3.049(4) Å; N6···O4$^{\#3}$, 3.219(3) Å; N6···O6$^{\#3}$, 3.227(3) Å, shown in Table 4). In this structure, there are two obvious layers (layer A in Fig. 4a and b) which are formed by TST^{3-} groups via those SO_3···H–N bonds, and the planar $Co2(phen)_2$ groups (layer B in Fig. 4a) are splinted in the two TST layers via the coordination and π–π interaction (3.41 Å). The 2D structures are further held together through the face-to-face (3.55 Å, 3.47 Å) and point-to-face (3.62 Å) interactions of *cis*-$Co1(phen)_2(H_2O)$ groups (layer C in Fig. 4a and c) which present beautiful and regular 1D chains, as shown in Fig. 4c. Most of uncoordinated water oxygen atoms are disordered, so that the existence of abundant hydrogen bonds formed by them is not discussed herein.

3.2.4. *Hetero-trinuclear cluster* $[Co_2Cu(phen)_6(H_2O)_2(TST)_2]\cdot 10H_2O$ **3**

The X-ray data of complex **3** show that there are also three metal centers in one molecule, and the ICP-AES test

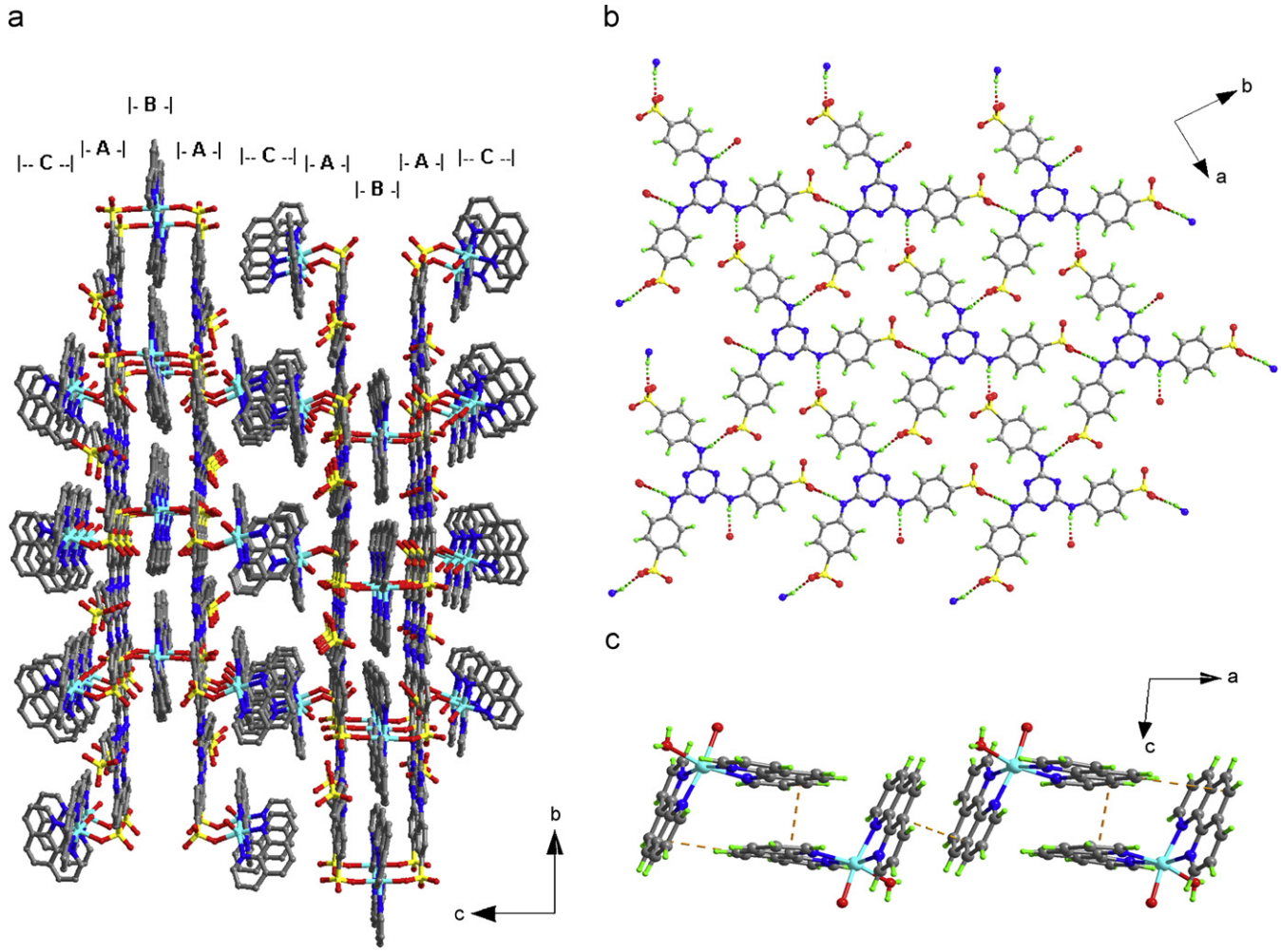

Fig. 4. (a) Packing structure looking down along *a*-axis in **2**, showing the A, B, and C layered structure. Solvent water molecules and hydrogen atoms were omitted for clarity. (b) The H-bonded layer A formed by TST ligands. (c) The 1D chain of *cis*-$Co(phen)_2$ groups in layer C, formed via π–π interactions.

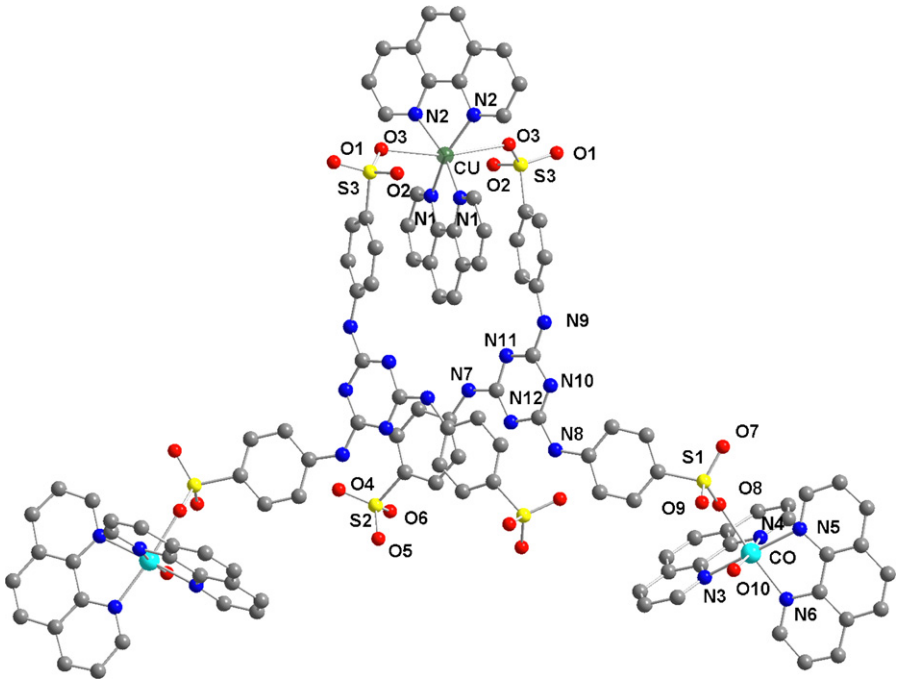

Fig. 5. The hetero-polynuclear cluster in **3**. Solvent water molecules and hydrogen atoms were omitted for clarity.

affirms that two of them are Co atoms and the other one is Cu atom. The obvious Jahn–Teller distorted metal center, which is localized on the crystallographic C_2 symmetry axis, should be the Cu(II) atom and the coordination environment of the other two metal centers shows that they are Co(II) atoms, which is similar to *cis*-Co(phen)$_2$O$_2$ units in complexes **1**, **2** and prior reports [25–30].

There is only one crystal structure containing *trans*-Cu(phen)$_2$O$_2$ unit has been reported [31]. Compared to the *trans*-Co(phen)$_2$O$_2$ unit in **2**, the distance of Cu–O(SO$_3$), 2.868(5) Å is quite long due to the Jahn–Teller effect. There is an angle of 28.5° between two phen groups in the *trans*-Cu(phen)$_2$O$_2$ unlike the nearly planar motif in **2**. The intramolecular connection of another trinuclear complex **3** is similar to that in **2**. However, the relative space locations and stacking mode of the TST^{3-} and Co/Cu(phen)$_2$ groups are quite different from that in **2** as shown in Fig. 5. The two phenyl rings of TST^{3-} ligands stack (3.55 Å) on the middle ring of the phen group in *trans*-Cu(phen)$_2$O$_2$ group, not the side ring as that in **2**, and the two TST^{3-} ligands have more overlap than that in **2**.

An extended 2D structure is also constructed via SO$_3$···H–N bonds (N8···O3$^{\#2}$, 3.216(3) Å; N9···O6$^{\#3}$, 2.939(3) Å, shown in Table 5) but in a different stacking mode between TST^{3-} (layer A in Fig. 6) and *trans*-Cu(phen)$_2$ groups (layer B in Fig. 6) comparing to those in **2**. The 2D structures are further held together through intermolecular π–π interactions (3.22 Å) between *cis*-Co(phen)$_2$O$_2$ units and coordinated sulfopheny groups, which also presents a regular π–π 1D chains (layer C in Fig. 6). Another interesting thing is that in this crystal structure SO$_3$ groups and aqua ligands form a hydrophilic space that hosts a tetramer H-bonded water cluster and a beautiful 16-atom O cluster is constructed by the oxygen atoms from these water clusters, SO$_3$ groups and aqua ligands, presenting an attractive motif with three 6-membered rings, middle of which is nearly a perfect hexagon as shown in Fig. 7.

Table 5
Hydrogen bonding interactions (unit: Å and deg) in **3**

D–H···A	D–H	H···A	D···A	D–H···A
N7–H7A···O11$^{\#1}$	0.86	2.29	3.151(5)	173.8
N8–H8A···O3$^{\#2}$	0.86	2.36	3.216(3)	177.1
N9–H9A···O6$^{\#3}$	0.86	2.10	2.939(3)	165.1
O10–H10A···O9	0.82	1.98	2.747(3)	156.5
O10–H10B···O12$^{\#6}$	0.898(2)	1.962(3)	2.815(4)	158.0(2)
O11–H11B···O9	1.035(3)	1.692(2)	2.697(4)	162.3(3)
O12–H12B···O2$^{\#2}$	0.885(3)	2.025(2)	2.873(4)	160.1(2)
O12–H12A···O13$^{\#5}$	0.987(4)	1.862(4)	2.761(6)	150.0(2)
O13–H13B···O14	0.915(4)	1.923(4)	2.824(5)	167.8(2)
O13–H13A···O5$^{\#7}$	0.946(3)	2.051(3)	2.944(4)	156.8(2)
O14–H14A···O11$^{\#4}$	1.017(3)	1.936(4)	2.912(5)	159.7(2)
O14–H14B···O5$^{\#5}$	0.924(4)	1.930(3)	2.838(5)	167.1(2)
O15–H15B···O1$^{\#2}$	1.099(5)	1.832(4)	2.927(6)	173.6(3)

Symmetry code: (#1) x,–y, z–$\frac{1}{2}$; (#2)x, $y+1$,z; (#3)x, –y, $z+\frac{1}{2}$; (#4) –$x+1$, y, –$z+\frac{3}{2}$; (#5)–$x+1$,–$y+1$, –$z+1$; (#6)x, –$y+1$, $z+\frac{1}{2}$; (#7)x–1, y,z.

3.2.5. *Behaviors of TST ligand in supramolecular architectures*

Only the HTST^{2-} in **1** adopts the φ-conformation and the TST^{3-} groups in **2** and **3** appear in the Δ-conformation, which is different with the Aakeroy's report [32] about a

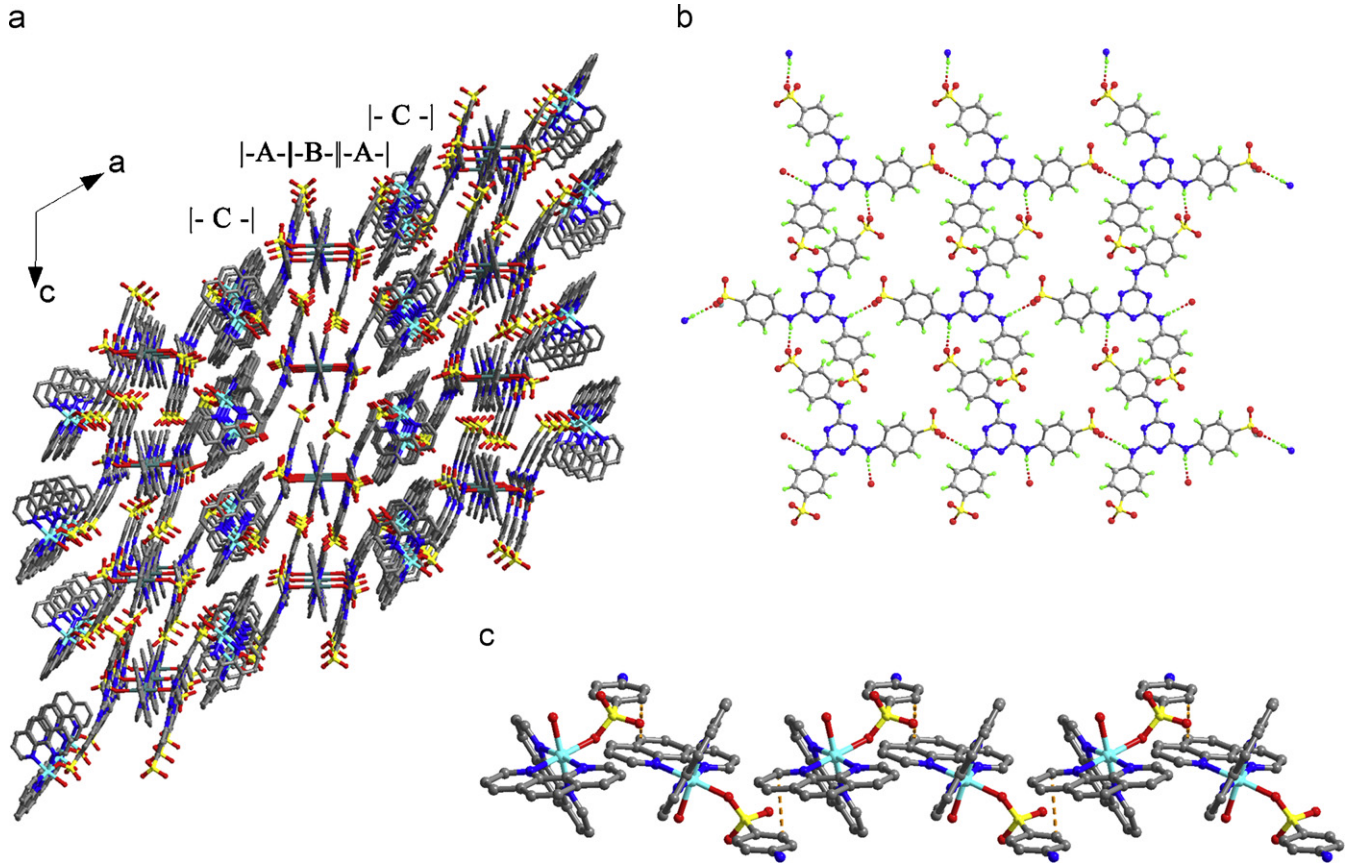

Fig. 6. (a) Packing structure looking down along *b*-axis in **2**, showing the A, B, and C layered structure. Solvent water molecules and hydrogen atoms were omitted for clarity. (b) The H-bonded layer A formed by TST ligands. (c) The 1D chain of *cis*-Co(phen)$_2$O$_2$ groups in layer C, formed via π–π interaction.

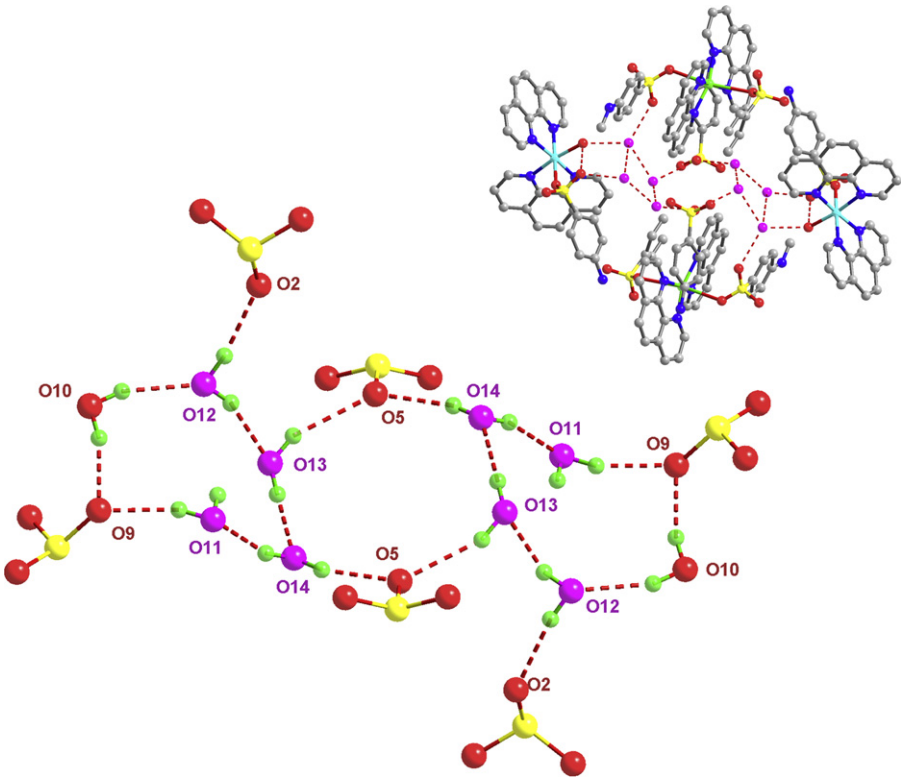

Fig. 7. The 16-atom O cluster, constructed by oxygen atoms from tetramer water clusters (pink), SO_3 groups, and aqua ligands.

flexible tri-carboxylic acid, 2,4,6-tris-(4-Carboxyphenoxy)-1,3,5-triazine. As a trimesic ligand, TST groups form no high symmetry structure in these work. But a 1D TST chain and two 2D TST networks are constructed in these three complexes via intermolecular H-bonds between SO_3 and N–H groups as shown in Fig. 8. In these structures, the SO_3 groups act as H-bond acceptors and the three N–H groups of a TST ligand play as an H-bond donor center. In 1D TST chain of complex **1**, only one SO_3 group of TST ligand is employed to form H-bonds. Then when all of the three SO_3 groups form H-bonds in TST layer of complex **2**, a trigonal H-bonded network is constructed. In complex **3**, a grid TST network is constructed via H-bonds formed by two SO_3 groups of TST ligand.

Three complexes were all constructed in aqueous solution via the weak coordination interactions of sulfonates in HTST/TST ligands toward the Co(II)/Cu(II) of $M(phen)_2^{2+}$ cations and the fact is demonstrated that tailoring the coordination environments of Co(II)/Cu(II) with phen groups is efficient for TST groups to compete with water molecules. However, it was failed to obtain polymer crystals containing TST and $Co/Cu(phen)_2^{2+}$ blocks, though many experimental methods have been tried.

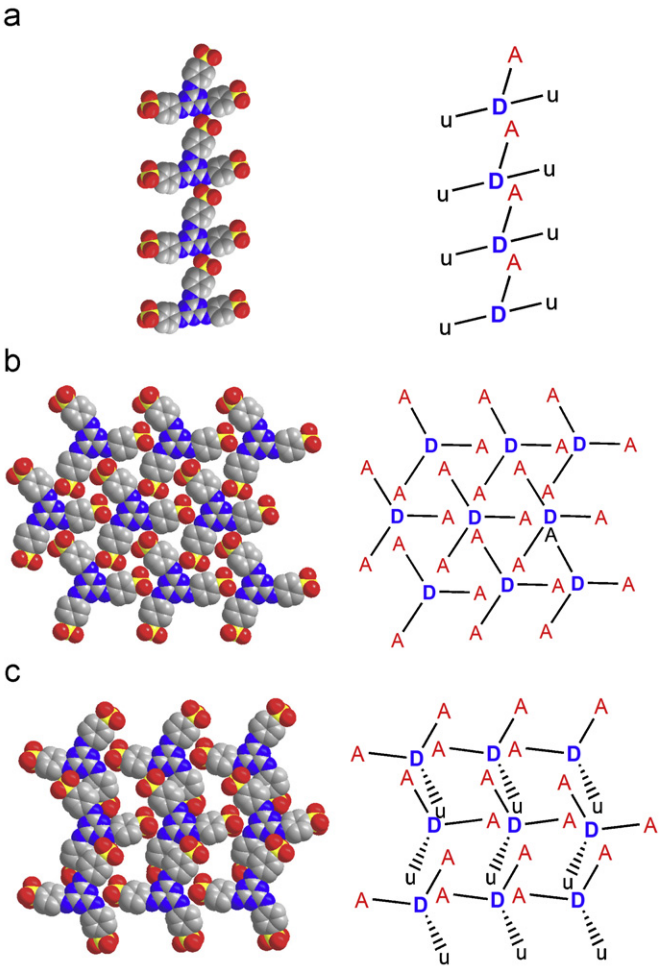

Fig. 8. H-bonded TST structures and their topology view in the complexes. (A: SO_3 groups which act as H-bond acceptors; D: H-bond donor centers; u: SO_3 groups which do not form H-bond with other TST ligands.) (a) The 1D chain in **1**; (b) The 2D trigonal network in **2**; (c) The 2D grid network in **3**.

3.3. *Thermal analyses of **1**, **2**, and **3***

TGA of 1, 2, and 3 show weight losses of 5.5%, 6.7%, and 7.9% before 200 °C, respectively (Fig. 9), which are close to the theoretical values of 5.1%, 6.2%, and 8.1% for the losses of water molecules. The degradations of the complexes are, respectively, at 380–600 °C, 400–580 °C, and 340–540 °C. When heated to 700 °C, the total weight losses of the three complexes are, respectively, 49%, 46%, and 52%.

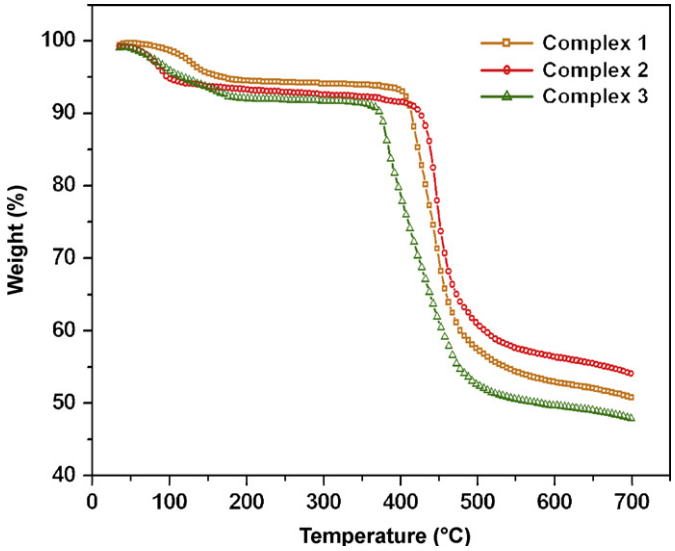

Fig. 9. TGA curves of **1**, **2**, and **3**.

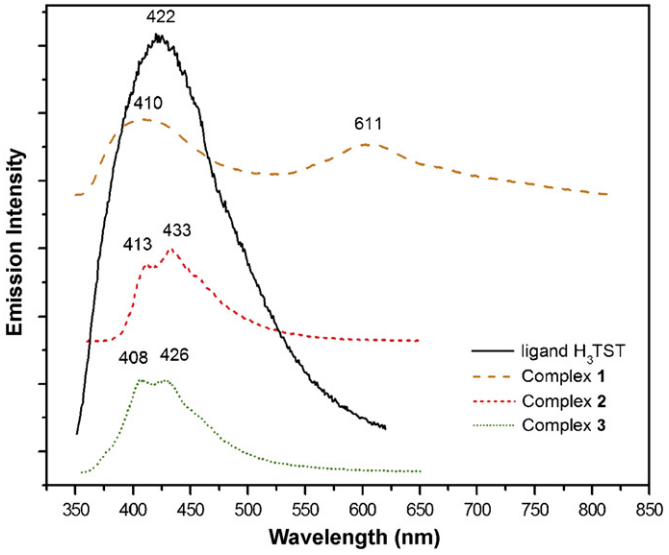

Fig. 10. Solid-state emission spectra of organic $H_3TST \cdot 7H_2O$ (solid line) and complexes **1**, **2**, and **3** (dash, short dash, and short dot lines, respectively) at room temperature.

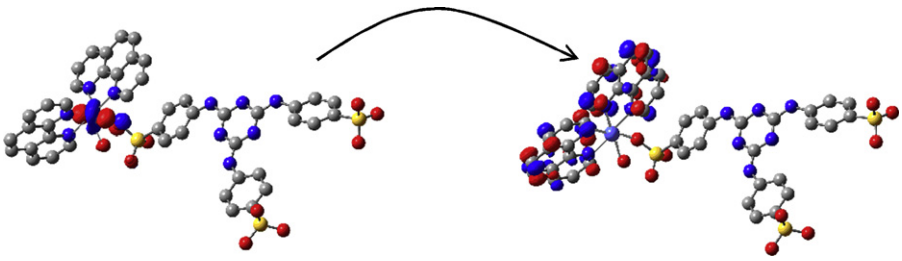

Fig. 11. Illustration of orbital transitions involved in the charge-transfer process.

3.4. Photoluminescent properties of *1*, *2*, and *3*

The emission spectrum of **1** exhibited two separate peaks at 410 and 611 nm, while the complexes **2** and **3** only had two shoulder peaks, 413 and 433 nm for **2**, 408 and 426 nm for **3** as shown in Fig. 10. The peaks in the region from 400 to 450 nm should be assigned to ILCT (intraligand charge-transfer) because the similar emission peak (422 nm) was also observed in emission spectrum of free ligand H_3TST. The second emission peak (611 nm) of **1** probably derives from LMCT (ligand-to-metal charge transfer). The lower energy of LMCT excited state causes red shifts in emission spectrum of **1** comparing to the free H_3TST. In complexes **2** and **3**, this LMCT may be quenched when the TST ligand coordinates to another metal center, *trans*-Co/Cu(phen)$_2$, as other studies reported [33].

3.5. Nonlinear optical property of *1*

It was reported that many dipolar metal complexes have second-order NLO properties [34]. The dipolar molecule structure of complex **1** also attracts our interest, and in solution its hyperpolarizability value has been measured and calculated.

The molecular first hyperpolarizability (β) of complex **1** was determined to 75×10^{-30} esu by means of the Hyper Rayleigh Scattering (HRS) technique at the laser radiation of 1.064 μm in DMSO solution. The extrapolated static β_0 was about 13×10^{-30} esu by using TLM. This β value is notably large among the cobalt coordination complexes.

The DFT calculation on the molecular hyperpolarizability of complex **1** well produced the HRS measurement with the calculated static β_0 value of 52×10^{-30} esu. Furthermore, the theoretical analysis revealed the MLCT (metal-to-ligand charge transfer) origin of the second-order NLO property. Shown in Fig. 11, the β-related CT mainly involved the excitation transition from the *d* orbitals of cobalt to the conjugated π^* orbitals of (phen)$_2$ moieties.

4. Conclusion

Three complexes with mononuclear, trinuclear, and hetero-trinuclear structure, respectively, have been constructed via controlling the base content of reaction environment and introducing hetero-metal building blocks Co(II)/Cu(II)(phen)$_2$ into the reaction. The flexible and trimesic structure of TST do created more opportunity for the construction of supramolecular architectures through weak coordination bonds, H-bonds and even π–π interactions, representing its potential capability in the design of crystal materials. As a second ligand, phen shows its tailoring ability in cooperation with sulfonate ligand and in the construction of poly- and hetero-nuclear complexes.

Acknowledgments

We gratefully acknowledge the financial supports of "973" Program (2007CB815307), MOST Project (2006DFA43020), Natural Science Foundation of China (20573114), and Project of Fujian province (2007F3115).

References

[1] A. Majumder, V. Gramlich, G.M. Rosair, S.R. Batten, J.D. Masuda, M.S. El Fallah, J. Ribas, J.P. Sutter, C. Desplanches, S. Mitra, Cryst. Growth Des. 6 (2006) 2355.
[2] X. Shi, G.S. Zhu, X.H. Wang, G.H. Li, Q.R. Fang, G. Wu, T. Ge, M. Xue, X.J. Zhao, R.W. Wang, S.L. Qiu, Cryst. Growth Des. 5 (2005) 207.
[3] H.W. Roesky, M. Andruh, Coord. Chem. Rev. 236 (2003) 91.
[4] J.Y. Lu, Coord. Chem. Rev. 246 (2003) 327.
[5] R.H. Wang, F.L. Jiang, Y.F. Zhou, L. Han, M.C. Hong, Inorg. Chim. Acta 358 (2005) 545.
[6] C. Ruiz-Perez, P. Lorenzo-Luis, M. Hernandez-Molina, M.M. Laz, F.S. Delgado, P. Gili, M. Julve, Eur. J. Inorg. Chem. (2004) 3873.
[7] D. Braga, L. Brammer, N.R. Champness, Cryst. Eng. Commun. 7 (1) (2005) 1.
[8] D.J. Hoffart, A.P. Cote, G.K.H. Shimizu, Inorg. Chem. 42 (2003) 8603.
[9] A.P. Cote, G.K.H. Shimizu, Inorg. Chem. 43 (2004) 6663.
[10] J.S. Zhou, J.W. Cai, L. Wang, S.W. Ng, J. Chem. Soc. Dalton Trans. (2004) 1493.
[11] S.L. Zheng, M.L. Tong, X.M. Chen, S.W. Ng, J. Chem. Soc., Dalton Trans. (2002) 360.
[12] J.W. Cai, C.H. Chen, C.Z. Liao, J.H. Yao, X.P. Hu, X.M. Chen, J. Chem. Soc. Dalton Trans. (2001) 1137.
[13] J.W. Cai, C.H. Chen, C.Z. Liao, X.L. Feng, X.M. Chen, J. Chem. Soc. Dalton Trans. (2001) 2370.
[14] C.H. Chen, J.W. Cai, C.Z. Liao, X.L. Feng, X.M. Chen, S.W. Ng, Inorg. Chem. 41 (2002) 4967.
[15] A.H. Mahmoudkhani, A.P. Cote, G.K.H. Shimizu, Chem. Commun. (2004) 2678.
[16] A.P. Cote, M.J. Ferguson, K.A. Khan, G.D. Enright, A.D. Kulynych, S.A. Dalrymple, G.K.H. Shimizu, Inorg. Chem. 41 (2002) 287.
[17] (a) S.A. Dalrymple, M. Parvez, G.K.H. Shimizu, Chem. Commun. (2001) 2672;

(b) S.A. Dalrymple, M. Parvez, G.K.H. Shimizu, Inorg. Chem. 41 (2002) 6986;
(c) S.A. Dalrymple, G.K.H. Shimizu, Supramol. Chem. 15 (2003) 591;
(d) S.A. Dalrymple, G.K.H. Shimizu, Chem. Eur. J. 8 (2002) 3010.
[18] (a) G.M. Sheldrick, SHELXS 97, Program for the Solution of Crystal Structures, University of Gottingen, Gottingen, Germany, 1997;
(b) G.M. Sheldrick, SHELXL 97, Program for the Refinement of Crystal Structures, University of Gottingen, Gottingen, Germany, 1997.
[19] M.J. Frisch, G.W. Trucks, et al., Gaussian 03, Revision B.04, Gaussian Inc., Wallingford, CT, 2004.
[20] S.J. Cyvin, J.E. Rauch, J.C. Decius, J. Chem. Phys. 43 (1965) 4083.
[21] J.T. Thurston, J.R. Dudley, D.W. Kaiser, I. Hechenbleikner, F.C. Schaefer, D. Holm-Hansen, J. Am. Chem. Soc. 73 (1951) 2981.
[22] V.R. Thalladi, S. Brasselet, H.-C. Weiss, D. Blaser, A.K. Katz, H.L. Carrell, R. Boese, J. Zyss, A. Nangia, G.R. Desiraju, J. Am. Chem. Soc. 120 (1998) 2563.
[23] R.K.R. Jetti, P.K. Thallapally, F. Xue, T.C.W. Mak, A. Nangia, Tetrahedron 56 (2000) 6707.
[24] H.A. Jahn, E. Teller, Proc. R. Soc. London Ser. A 161 (1937) 220.
[25] D. Poleti, L. Karanovic, G.A. Bogdanovic, A. Spasojevic-de Bire, Acta Crystallogr. Sect. C Cryst.Struct.Commun. 55 (1999) 2061.
[26] J. Yang, J.F. Ma, D.M. Wu, L.P. Guo, J.F. Liu, J. Mol. Struct. 657 (2003) 333.
[27] F. Li, L. Xu, Y. Wei, E. Wang, Inorg. Chem. Commun. 8 (2005) 263.
[28] R.B. Fu, S.M. Hu, Z.Y. Fu, J.J. Zhang, X.T. Wu, New J. Chem. 27 (2003) 230.
[29] V.T. Yilmaz, S. Demir, O. Andac, W.T. Harrison, J. Coord. Chem. 55 (2002) 863.
[30] S.F. Lai, C.Y. Cheng, K.J. Lin, Chem. Commun. (2001) 1082.
[31] E. Freire, S. Baggio, R. Baggio, M.T. Garland, Acta Crystallogr. Sect. C Cryst. Struct. Commun. 54 (1998) 464.
[32] C.B. Aakeroy, J. Desper, J.F. Urbina, Cryst. Eng. Commun. 7 (2005) 193.
[33] (a) Y. Liu, S. Zhang, Q. Miao, L. Zheng, L. Zong, Y. Cheng, Macromolecules 40 (2007) 4839;
(b) A.P. de Silva, H.Q.N. Gunaratne, T. Gunnlaugsson, A.J.M. Huxley, C.P. McCoy, J.T. Rademacher, T.E. Rice, Chem. Rev. 97 (1997) 1515.
[34] S.D. Bella, Chem. Soc. Rev. 30 (2001) 355.